Article:
Kirkby, MJ (2018) A conceptual model for physical and chemical soil profile evolution. Geoderma, 331. pp. 121-130. ISSN: 0016-7061

https://doi.org/10.1016/j.geoderma.2018.06.009

A conceptual model for physical and chemical soil profile evolution

M.J. Kirkby, School of Geography, University of Leeds, UK.

m.j.kirkby@leeds.ac.uk

Abstract

A simplified soil model is presented for evolution of the mineral soil profile. The model provides a compromise between highly empirical models and highly mechanistic/ geochemical models, and represents some of the main features of observed profiles, with features that can be identified with 'A', 'B' and 'C' horizons. The model is responsive to a range of global environments, which can be represented through climate and parent material parameters. In many cases there is an almost single-valued relationship between surface weathering and soil depth, allowing further simplification of the model, and allowing it to be included within a parsimonious landform evolution models. A key parameter and assumption of the model is the degree of weathering below which no further solution occurs, which limits the maximum extent of soil development. This is speculatively linked to CO_2 turnover rates and the degree of aridity.

Keywords

Soil profile; modelling; bioturbation; weathering

Introduction: proposed model framework

Hydrological, biological, chemical and mechanical processes take place throughout the critical zone (Figure 1), interacting at a wide range of temporal scales, and together driving evolution of the soil / regolith profile. Over time, weathering introduces material into the base of the profile, while geomorphic processes transport material downslope, progressively eroding the surface of the land. These processes interact, slower weathering, for example, producing coarser material that is eroded more slowly. Rates of production and removal may be out of balance for millions of years, leading to either indefinite accumulation of soil or stripping to parent material, but in many cases there is an approach to a quasi-equilibrium with a finite depth of soil.

In this paper, processes of soil formation have been simplified to provide a tentative theoretical framework, providing a conceptual model of soil profile evolution. This builds on, and expands, prior work (Carson and Kirkby, 1972; Kirkby 1977, 1985a), and has been informed by the many and diverse soil evolution models in the literature (e.g. Minasny & McBratney 1999, 2001; Finke & Hutson 2008; Gabet & Mudd,2009; Opolot & Finke, 2015). A number of simplifying assumptions have been made to keep the model relatively simple, particularly with respect to the geochemical evolution of the soil, although some can, in principle, be relaxed. A high priority has been to include as many significant interactions between the processes acting within the profile as possible, and particularly those between the evolving profile and soil hydrology. The

necessary resulting simplifications have, hopefully, provided some gains in understanding but also consequential sacrifices in rigour.

Early concepts of soil development express the evolving balance of physical and chemical denudation (Carson & Kirkby, 1972, p 265), leading either to an equilibrium in which the degree of weathering at the surface is a function of the balance between the two forms of denudation, or to indefinite deepening of the soil profile. The increase in soil depth is given by the difference between the rate of weathering and the rate of erosion, corrected for the degree of weathering of the surface material. The rudimentary model proposed by Minasny and McBratney (1996, 2001) takes account of a depth-dependent weathering rate and a surface-controlled erosion rate to develop the profile model, additionally taking account of changes in bulk density as weathering proceeds. Brimhall & Dietrich (1987) combine this approach with a much more sophisticated geochemical analysis to show how recalcitrant soil components (Fe and Al) may accumulate as hardpans or laterites as silica is preferentially removed due to its greater solubility.

Hoosbeek & Bryant (1994), Lebedeva et al(2010) and Li at al (2014) make use of similar advection-dispersion equations for the movement of solutes to those used by Kirkby (1985a) and van Genuchten & Wierenga (1986), and estimate solute concentrations by appealing to chemical equilibrium between water and solid mineral phases.

Willgoose and his group (Cohen et al, 2010; Welivitya et al, 2016) have focussed on the physical breakdown of material into progressively finer fractions, and the accumulation of an armour layer at the surface as water erosion winnows fines to progressively concentrate the coarser material. In the mARM3D model alternative depth-dependent weathering functions are combined with the comminution model to provide a valuable model for critical zones for which physical breakdown is the dominant process. These models have also been coupled with landscape evolution models to generate downslope catenas as the landform as a whole evolves.

Other soil profile models has made a much more detailed analysis of chemical processes, generally using kinetic equations to describe rates of solution and solution products for different constituent minerals. Examples of such models are the WITCH model (Goddéris et al, 2006) and the SoilGen model (Opolot & Finke, 2015). These models also explicitly incorporate carbon cycling to provide relevant levels of CO_2 partial pressure in the soil, linking to RothC or ASPECTS to provide carbon cycling and outgassing. They also include some hydrology, allowing them to respond to the external environment. Due to their relative complexity, however, they are more difficult to couple with landscape evolution.

Vanwalleghem et al (2013) have created a model explicitly for coupling with landscape evolution (MILESD), dividing the soil profile and parent material into four layers to model movement of solutes and clay between layers, bounded by depth-dependent weathering of parent material and diffusive sediment transport at the surface. Carbon cycling and bioturbation are also significantly incorporated in exchanges between the upper layers. This approach represents

an advance on previous work through integration of hydrology and weathering into a simple and unified model structure that is compatible with landscape evolution models.

Because of the complexity of the processes operating in soils, and their interaction with surface sediment processes, all models represent compromises, emphasising some aspects and over-simplifying others. The present proposal provides no resolution from this dilemma, but offers an alternative approach which has some strengths, and allows further exploration of some internal linkages. Nevertheless it is recognised that carbon cycling is currently not included, and that changes in bulk have been assumed to be negligible, with loss of substance balanced by a corresponding reduction in density, an assumption that is, in some contexts, demonstrably false.

Here we make a number of major assumptions in order to simplify and generalise some of the processes involved in soil profile development. The first, and most important of these, is to combine all chemical constituents into a single term which expresses the degree of weathering, and is defined below. It is implicit in this assumption that weathering is a largely congruent process, so that, for a given parent material and physical environment there is an almost one-to-one relationship between degree of weathering and chemical composition, so that, for example, there is a single-valued relationship between degree of weathering and solute concentration. This relationship is analogous to the commonly used approximation that, at a site, there is a single-valued relationship between soil moisture storage and flow rate.

The second major assumption is that modifications in the rates of other processes can also be simply related to degree of weathering. This dependence has been applied implicitly to grain size distribution, and explicitly to the rate of surface sediment erosion (or as one control on the rate of sediment transport in a landscape context). The functional form of these relationships has usually been expressed here as a power law, with exponents reflecting qualitative rather than quantitative forms. The third assumption made is that solute concentrations in soil water are, on the time scales of profile development, in chemical equilibrium with the solid phase, so that concentrations are the product of a solubility that is the mass-weighted concentration of mineral solubilities in the weathered solid phase at a given degree of weathering, again expressible as a single valued function of the current local degree of weathering. This assumption reflects experimental work on silicates (Garrels & Christ, 1965; Bricker et al, 1968; Robinson & Stokes 1959), suggesting that equilibration occurs over periods of about 100 hours for silica, and somewhat longer for alumina: all periods that are short compared to the time scale for profile evolution.The fourth major assumption is that there is no change in volume as the soil weathers. This assumption has been used in a number of previous models (e.g. Lebedeva 2010) and is visibly supported by the presence of intact structures within saprolite, for at least some parent materials, but is not universally applicable, for example in limestones and podsols. The fifth major assumption is that, for a given environment and parent material, there is a maximum degree of weathering beyond which no further soil development occurs. This assumption is speculative, but is essential to the model. It is discussed briefly in the conclusions below.

Ignoring, initially, the organic horizons, a simple way to characterize the changing properties of the profile is by referring to the total loss of substance at any level, based on an analysis of all constituent minerals. If a hypothetical constituent that is assumed to be totally insoluble is increased in abundance by k times at some level in the profile relative to its abundance in the parent material, then the proportion, p, of rock substance at that level $1/k$. . In many cases, simple soil profiles can then be generalised as a sigmoid curve, with the proportion remaining, p, declining from 1.0 at depth in parent material, and falling to progressively lower values towards the surface as in the definition sketch of figure 2. In the absence of a non-arbitrary lower boundary, a generalised 'soil deficit', ζ ,can also usefully be defined as the total depth of material that would have to be replaced to restore the soil to its original, parent material, condition. This can be written:

$$\zeta = \int(1-p).dz \qquad (1)$$

where the integral is evaluated from the surface downwards, and ζ has the dimension of depth.. This generalisation is necessary since there is not a sharp boundary between soil and parent material. Where there is such a sharp boundary, with weathering at p^* above, then soil depth, $z = \zeta/(1-p^*)$.

A key variable is the value of p at the surface, p_s. Since, to a first approximation, mechanical loss takes place at the soil surface, a mass balance for the soil profile is:

$$\frac{d\zeta}{dt} = C - M.\frac{p_s}{1-p_s} \qquad (2)$$

If there is an equilibrium soil profile developed under constant rates of mechanical (M) and chemical (C) denudation,

$$p_s = M/(M+C) \qquad (3)$$

the state of weathering is also commonly summarised in the 'Chemical Depletion Ratio',

$$\text{CDR} = 1-p_s = C/(M+C) \text{ at soil equilibrium.} \qquad (4)$$

These relationships are fundamental to almost all soil profile models.

In this paper the processes of soil evolution are modelled in a simplified way, primarily in terms of the one dimensional profile of substance remaining, as sketched in figure 2. It is recognised, and here assumed, that, for different parent materials, the composition of the soil at different stages of weathering reflects both its mineral assemblage and its grain size composition, and that the concentration of solutes in soil water shows a different, but consistent, dependence on substance remaining at various stages.

A first, strongly simplifying, approximation to the course of weathering can be obtained by analysing rock minerals as a mixture of oxides, and assigning a constant solubility to each, without allowing for interactions as mineral composition changes. Over time, the most soluble components of the rock dissolve most rapidly, so that the composition of the weathered material concentrates the less soluble components, such as Iron and Aluminium oxides, and the average solubility of the remainder is reduced to reflect this change in composition. Table 1 and figure 3 illustrate this dependence for an idealised igneous rock. This approach, although ignoring the successive mineral assemblages as weathering proceeds, mirrors the overall course of weathering sufficiently for the present model, but is included here only as illlustrating the overall direction of the weathering sequence

For the present model, figure 3(c) illustrates the decrease in solubility as weathering proceeds. This will be represented in the model as a decrease with proportion remaining, falling to zero at a minimum proportion, p_0, representing the ultimate final achievable state of weathering. The proposed model is intended as one of reduced complexity, allowing readier linkage to landscape evolution models and, inevitably, greatly simplifying the geochemical relationships, which , for the purposes of the model, are summarised entirely through the assumed relationship between solute concentration and proportion remaining, encapsulated in equation (6) below or an alternative

Hydrological and Chemical Process representation

Figure 1 indicates the range of processes that have been incorporated into the model, which is driven by these processes within a mass balance framework that accounts for both water and soil substance, generally working implicitly with annual rather than seasonal or storm-based totals, although the time step varies to maintain computational stability. The hydrology is driven externally by precipitation and actual evapotranspiration (ET = E_A), the latter derived from potential ET and precipitation using a Budyko transformation (Arora, 2002). ET is assumed to decay exponentially with depth, based on an assumed average root depth z_E, giving a total ET demand below depth z of $E_A \exp(-z/z_E)$. In the present form of the model, ET is assumed to consist of water free of solutes, but may be modified to allow for the solute demands of the vegetation cover. Progressive weathering is currently assumed to take place without change of volume, so that soil porosity increases as (1-p), although with the facility to allow some percolation into intact parent material. At any depth z, the potential for lateral subsurface flow $q(z)$ is related to the porosity through the relationship $q(z) \sim (1-p)^2$ (Terzaghi & Peck 1967). Actual downward percolation is then estimated as the lesser of the two quantities, each with the dimension of $mm.a^{-1}$ [LT^{-1}].

Rainfall R depleted by accumulated ET above this depth: $= R - E_A(1 - \exp(-z/z_E)$ (5a)

Potential for lateral flow together with ET demand below level z : $= \int q(z) + E_A \exp(-z/z_E)$ (5b)

The contribution to lateral sub-surface flow from within the soil profile is then zero if the first expression (equation 5a) is the lesser (commonly near the surface), and is q(z) if the latter expression is less. This condition occurs below the saturated level for a humid climate, but not normally under arid conditions, and increases with hillslope profile convexity. This contribution from the individual soil profile to lateral subsurface flow (down the hillslope) is assumed to carry away solutes at their equilibrium concentration within the soil water. With increasing depth and associated reduction in weathering, losses by advection will also become progressively smaller. The choice of this hydrological sub-model allows the soil hydrology to change dynamically in response to climate and the progressive evolution of the soil profile, and it is representation of this interaction that provides an important driver of the proposed model. It is implicit in this assumption that the soil profile considered is identical to those above and below

it, an assumption that is most clooely met for a uniform convex hilltop. For other contexts, the present one-dimensional analysis should be nested within an analysis that represents the entire hillslope catena. These issues have been discussed, though not fully resolved, by Willgoose (2018).

Soil water is assumed, in the model, to come to chemical equilibrium with the constituents of the solid phase of weathered material, and to do so over a time span that is short relative to the rate of evolution of the soil profile. The local concentration in the soil water is then the product of the solubility of the weathered material and the proportion of substance remaining, both estimated at the level of interest within the profile. In the model, the assumed relationship between concentration and proportion present, *c(p*), has been given the form:

$$c(p) = c_* \left(\frac{p-p_0}{1-p_0}\right)^{0.5} \quad (6)$$

Where c_* is the solute concentration in parent material, and p_0 is the ultimate state beyond which weathering cannot proceed. This relationship is taken to incorporate dependence on pH and pCO_2 in the context of the weathering sequence for a particular parent material. It is noted that this relationship differs appreciable from the curve shown in figure 3c, with a much more abrupt cut-off as p_0 is approached. This difference reflects the observation that observed deep soil profiles appear to show the persistence of a lower limit for weathering, which may take values of 0.4 for laterites (e.g. Hamdan & Burnham, 1996), but much higher values of around 0.8 in Sierra Nevada (CA) granites (Riebe et al, 2003). This lower limit appears to be a strong control in practice, although one that is unexplained by the simple linear theory shown in figure 3 and Table 1. This issue is addressed further below. The form of equation 6 with an exponent of 0.5 has been chosen to provide a sharp decrease in solubility as p_0 is approached, but is, to some extent, arbitrary.

Two key processes are represented in the model to allow exchange and removal of solutes, namely diffusion and advection. Diffusion occurs in two important ways. First ionic diffusion dominates the region close to parent material, where there is little exchange of water, so that differences in solute concentration drive diffusion of ions, leading to a net migration away from parent material into the body of the soil. Diffusion coefficients for different ions range over about one order of magnitude. In free water, values are typically in the range 200-2,000 $cm^2.a^{-1}$ (Robinson and Stokes, 1959), but allowing for tortuous flow in soil pores, effective values may be two orders of magnitude less. Here the value of 100 $cm^2.a^{-1}$ is adopted for all ions. Near a tight parent material, where there is no significant downward percolation (and solute advection) through the rock, ionic diffusion is the dominant solute transfer process acting. In isolation this will be seen to give a soil profile of the form:

$$p = 1-\exp(-z/z_0) \quad (7)$$

for a suitable scaling constant z_0. The rates on soil development produced by ionic diffusion are rather slow, since movement is only of the ions, which are always in relatively low (1-1000 $mg.l^{-1}$) concentrations within the soil water.

Diffusion is also active near the soil surface, where bioturbation, acting through frost-heave, earthworm burrows, tree-throw etc, drives random exchanges that turn over the entire mineral soil and organic matter (Gabet et al, 2003). This bio-diffusion is responsible for creating a bulk density and porosity profile near the soil surface, and for driving the seasonal soil creep that is responsible for many hilltop convexities (Gilbert 1909). In both cases, net outward diffusion towards the surface is balanced by settlement under gravity. Measured diffusion rates (Kirkby, 1967; Johnson et al, 2014) of 1-100 $cm^2.a^{-1}$ are comparable to those for ionic diffusion, but are responsible for moving much greater (10^3-10^6 times) volumes of material, since the entire soil contents are being exchanged. Since this process is, by far, the most rapid in the context of evolving mineral soil, its effect is to produce a zone of thorough mixing and homogenisation of the mineral soil. However these rates of exchange are comparable to rates of organic matter production and decomposition, so that the near-surface zone retains strong horizonation of organic soil constituents.

Advection is driven by flowing water that is carrying solutes. Solutes are dissolved in the water, and are assumed to come to chemical equilibrium with the solid phase composition in times short compared to those required for significant soil evolution. Experiments suggest that the relevant period for substantial equilibration is a few days (Bricker et al, 1968), although some reactions are much slower than this. Only for overland flow runoff may reaction times be significantly shorter, perhaps reducing weathering rates at the surface (Gabet & Mudd, 2009): this effect is neglected here. Waters percolates downwards at a decreasing rate as porosity and hydraulic conductivity decline, is diverted laterally as a contribution to downslope subsurface flow, and is lost to evapotranspiration. Downward and lateral flow contributions are assumed to advect water at the local solute concentration, while ET is assumed to respond to plant requirements, and is here assumed to be free of solutes. The diversion of clean water for evapotranspiration can have the effect of increasing concentration of the remaining dissolved material in the remaining water, but this process is limited as concentrations reach saturation, beyond which further solutes are precipitated back into the solid phase.

A Steady State Solution

As an introduction to the dynamics of the model system, a straightforward analytical solution can be obtained if the following assumptions are made: no bioturbation; constant solute concentration (replacing equation 5 above); a net downward water flux proportional to (1-p) representing the increase in permeability as weathering proceeds; and a constant rate of material loss at the surface through erosion.

With these assumptions, the mass balance equation for the soil profile is:

$$\frac{\partial p}{\partial t} = \frac{\partial}{\partial z}\left[Qpc - \frac{\partial}{\partial z}(pcD_I)\right] \quad (8)$$

where both sides of the equation have units of [T^{-1}]

z is depth below the surface (mm),

Q is the downward water flux (mm.a-1),

and D_I is the ionic diffusion rate ($mm^2.a^{-1}$)

Assuming that the downward water flux is $R(1-p)$, where R is net rainfall, and that, in the steady state, the frame of reference is moving at rate v, then, setting

$p_0 = v/(Rc)$, $z_0 = D_I/[R(1-p_0)]$ and $\alpha = (1-p_s)/(p_s-p_0)$, the steady state solution is:

$$p = \frac{1+p_0\alpha\exp(-\frac{z}{z_0})}{1+\alpha\exp(-\frac{z}{z_0})} \quad (9)$$

which is a sigmoid curve for the dimensionless proportion p, with the general form shown in figure 2, for which $p \to p_0$ as $z \to -\infty$; $p = p_s$ at $z = 0$ and $p \to 1$ as $z \to +\infty$. An example of the associated fluxes and gains/losses is shown in figure 4. If bioturbation is introduced into this solution, there is a region of almost constant mineral composition that extends throughout the depth of biological mixing, but very little flux within this region because any slight perturbation is quickly removed by the rapidity of diffusion.

Computer simulation model

In order to address non-equilibrium conditions, Equation (8) should be modified to include bioturbation effects, and an additional equation is required for the hydrological mass balance.

Equation (8) then becomes:

$$\frac{\partial p}{\partial t} = \frac{\partial}{\partial z}\left[Qpc - \frac{\partial}{\partial z}(pcD_I + pD_B)\right] \quad (10)$$

where D_B is the rate of diffusion by bioturbation..

Water balance down the profile is given by

$$-\frac{\partial Q_v}{\partial z} = E(z) + q(z) \qquad (11)$$

where Q_v is the vertical downward water flux,carrying solutes at concentration c(z)

E(z) is the lateral ET flux at depth z, carrying only solutes to meet plant requirements

q(z) is the contribution, across the soil profile to lateral subsurface flow, carrying solutes at c(z). This is determined by equation (5) above. It is generally zero near the surface, and increases with hillslope profile convexity and with increased weathering.

The concentration c at any level now follows equations (10) and (11) rather than remaining constant, except that the ET stream is here assumed to be of pure water. A second diffusion term has been added to equation (10), representing bioturbation of the entire soil mass near the surface. The Biological diffusion and ET are each assumed to decay exponentially with depth, each with its own scale depth that is treated as a model input. Finally the rate of mechanical removal for weathered soil, M_0, is taken as an input variable that is considered to reflects the landscape morphology in which the modelled soil profile is set. However, it is recognised that removal rate also depends on the state of soil weathering, tending to zero for intact unweathered parent material, with a coupling observed by Riebe at al (2003) and modelled by Gabet & Mudd (2009). Here it is recognised that mechanical removal rates decrease sharply for almost unweathered soils, and this qualitative observation is expressed quantitatively in the present model in the assumed form:

$$M = M_0(1 - p_s)^{0.1} \qquad (12)$$

where M_0 is the mechanical erosion on fully weathered material (p_s=0)

This expression supresses removal to 80% for p_s=0.9, and to 60% for p_s=0.99, so that it has little effect except in the initial evolution of parent material surfaces. This approach implicitly takes some account of the physical breakdown of material, the dominant component of the Cohen et al (2009) mARM model applied to weathering on mine waste rock. The observed coupling also requires that chemical weathering rates are reduced as the soil thickness increases, as documented by Heimsath et al (1997) through cosmogenic dating. This relationship has not been included in the model as an explicit assumption, but is seen as an output of the model, reflecting the lesser circulation of water as soil deepens. Table 2 summarises the parameters required to define and run the model, indicating the ranges of values that have been applied.

Figure 5 shows an example model output for a humid region. It shows the development of a near-surface region of uniform concentration, dominated by bioturbation, and broadly corresponding with the 'A' horizon of the soil. Below, a weathering front develops, in which the proportion remaining increases rapidly with depth, leading to a region where there may be accumulation of material, as a result of concentration by loss of ET. This region, broadly corresponding to a 'B' horizon, becomes pronounced, as in the example shown, when the scale depth for ET is greater than the scale depth for bioturbation. Since biological activity influences both of these distributions, it is expected that they will be broadly similar. Below this zone of potential enrichment, ionic diffusion dominates to produce the 'C' horizon where weathering is gradually penetrating into parent material. For the same model run, figure 6 shows the relationship between solution rate and soil deficit (broadly equivalent to depth), an exponential decline similar to that measured by Heimsath et al (1997), in this case with a scale depth of approximately 80mm.

For a range of climates, defined by their precipitation and potential ET, figure 7 shows how the modelled soil depth evolves over time. The values on the right show the ratio of precipitation to Pot ET, which seems to control the overall course of evolution. In all cases the soil deficit develops at an accelerating rate initially, and finally settles down to an equilibrium value as the weathering rate falls to the imposed mechanical rate of denudation. These model runs suggest that, for the most arid climates, the evolution will be towards steady accumulation, corresponding, for example, to a soil with strong calcrete development.

Figure 8 illustrates how the modelled evolution converges towards its equilibrium state for a range of initial conditions that differ only in the initial rate of mechanical denudation, M_0. This corresponds to a set of slopes of different gradients, or to different points along the same slope profile. For high initial mechanical denudation rates, there is little chemical evolution, whereas, where mechanical denudation is low, there is substantial weathering, and profiles evolve asymptotically to a state where the state of surface weathering, p_s, is close to the final state of p_0. This curve is compatible with field data such as that presented by Riebe et al (2003), if it is assumed that weathering rate declines exponentially with soil depth.

For a set of solutions within the same weathering environment, but with different mechanical settings, such as those shown in figure 8, there appears to be a more or less single valued relationship between soil deficit, ζ and the proportion remaining at the surface, p_s. This is shown for this set of runs in figure 9. An empirical fit to the curve shown is

$$x = \exp\{\mathrm{A}\left[-3 + 3\exp\left(-\frac{\zeta}{4.3}\right) - \frac{\zeta}{4.3}\right]\} \qquad (13)$$

for constant A and where $x = (p_s - p_0)/(1 - p_0)$. This differs from the equivalent relationship found for the steady state solution of equation 9, which contains only the final term of equation 13.

The model has been set up here as one-dimensional, representing a single soil profile. The mass balance equations can be written in the forms

Total denudation: $\frac{dy}{dt} = -(C + M)$ (14)

Solute denudation: $\frac{d\zeta}{dt} = C - M\frac{1-p_s}{p_s}$. (15)

Where y*z* is the elevation of the soil surface.

With suitable expressions for the chemical and mechanical denudation rates, these equation can be solved, either analytically or computationally, but to do so requires an additional relationship, which may be considered as a 'rating curve' that connects soil deficit to the degree of surface weathering. Figure 9 and equation 11 suggest that this is a workable approach to provide a much simpler computational model, an example of which is shown in figure 10.

The potential value of this approach may be seen to be much greater if the soil model is embedded in a two- or three- dimensional landscape evolution model, with feedback between soil and landform evolution as sketched in figure 11. In this case the corresponding mass balance equations are:

Total material transport: $\frac{\partial y}{\partial t} = -\boldsymbol{\nabla}.(\boldsymbol{V} + \boldsymbol{S})$ (16)

Solute transport: $\frac{\partial \zeta}{\partial t} = -\boldsymbol{\nabla}.\left(\boldsymbol{V} - \boldsymbol{S}\frac{1-p_s}{p_s}\right)$ (17)

where **V** and **S** are respectively the vector solute and sediment transport at each point in the landscape and $\boldsymbol{\nabla}$ is the vector divergence operator. Similar equations must also be applied for the water balances. As for the 1-D case, a relationship of the form $\zeta = f(p_s)$ can be used to close the set of equations, subject to boundary & initial conditions. The viability of this approach, with a simpler soil model, has previously been demonstrated (Kirkby, 1985b).

Detailed behaviour in the bioturbation layers is not pursued here, but the homogenization of the mineral soil is accompanied by much greater changes in the soil organic matter, creating profiles of organic matter concentration and porosity/ bulk density. Outward diffusion by bioturbation is balanced by downward settlement under gravity. Organic matter, generated near the surface through leaf fall, root decay etc, decomposes and is mixed, predominantly downwards. The surface may also be subject to erosional stripping or the deposition of wind-blown material, providing near-surface interactions that are critical to 'A' horizon development but that may initially be ignored in the present context of mineral profile evolution.

p_0, the final product of weathering

It has been assumed above that weathering cannot, in a particular environment, proceed past a certain state, and this state has been represented in the model as an input parameter, p_0. It is widely observed that there is a global pattern of soil types, and there is a corresponding distribution for, p_0, the end point of mineral weathering. Any tentative suggestions here also assume constant climatic environments, so that they can best reflect conditions in areas where these have been stable for long enough to approach equilibrium soil conditions. It is tentatively suggested that the end point is associated with both aridity and soil CO_2 production. Aridity is closely linked to the ratio of potential ET to precipitation. High aridity is associated with accumulation of duricrusts, particularly calcrete, within the soil horizon, and so with high values of p_0. CO_2 production is associated with high rates of actual evapo-transpiration, and is associated with high rates of organic complexing with Fe and Al (Hernández-Soriano, 2012), which may limit their further dissolution, setting the value of p_0 in humid tropical

environments. Figure 12 sketches these regions on a diagram of annual precipitation and temperature, relating them to the index

$$\log(AE) + \log(r/R) \qquad (18)$$

where AE is estimated annual actual evapotranspiration, and r/R is the estimated ratio of runoff to precipitation. This diagram conforms with observed patterns, with laterites ($p_0 \sim 0.4$) in humid tropical areas, and the least weathered soils in semi-arid regions. It is acknowledged that these suggestions are highly speculative, with the mechanisms for such a relationship still unclear, and that there is scope for much further work on this topic.

Conclusions

It has been shown that a relatively simple model is able to capture many of the key essentials of soil profile development over time, and in response to a wide range of climatic evironments. It is acknowledged there is scope for much greater detail that involves specific mineralogy and weathering paths. It is also recognised that even the generalised path of weathering shows strong dependence on acidity (Ph), partial pressure of CO_2 (pCO_2) and reduction potential (Eh). Nevertheless the simple model is able to show realistic dependence on broad lithological and climatic controls in a way that has the potential to provide a broad-brush picture of global soil patterns in time and space. The relative simplicity also allows incorporation into landscape evolution models for 2-D or 3-D landscapes that retain soil profile evolution and dynamics in a meaningful, if simplified way.

It has been noted that the modelling requires defining a lower limit of weathering for an environment, and that there appears to be no satisfactory explanation for this phenomenon. There is weak evidence that this lower limit is connected with the interaction of mineral soils with organic soil components, but no clear mechanism.

References Cited

Arora, V.K.2002. The use of the aridity index to assess climate change effect on annual runoff. J. Hydrology, 265, 164-177.

. Bricker, G.P, Godfrey A.E.. Cleaves, & E.T 1968. Mineral-water interactions during the chemical weathering of silicates. Advances in Chemistry Series No 73: Trace inorganics in water, 128-142.

Brimhall. G.H. & Dietrich, W.E., 1987. Constitutive mass balance relations between chemical composition, volume, density, porosity, and strain in metasomatic hydrochemical systems: Results on weathering and pedogenesis. Geochimica et Cosmochimica Acta, 51, pp.567-87.

Carson M.A. and Kirkby, M.J. 1972. Hillslope Form & Process, CUP, 475pp.

Cohen, S. Willgoose G .and Hancock, G .2009. The mARM spatially distributed soil evolution model: A computationally efficient modeling framework and analysis of hillslope soil surface organization. Journal of Geophysical Research, 114, F03001, doi:10.1029/2008JF001214

Finke P.A. & Hutson J.L., 2008. Modelling soil genesis in calcareous loess. Geoderma 145, 462-479.

Gabet E.J.. Mudd, & S.M 2009. A theoretical model coupling chemical weathering rates with denudation rates. Geology 37, 151-154.

Gabet E.J.,. Reichman O.J &. Seabloom E.W, 2003. The Effects of Bioturbation on Soil Processes and Sediment Transport. Annu. Rev. Earth Planet. Sci. 2003. 31:249–73 doi: 10.1146/annurev.earth.31.100901.141314

Garrels R. M and. Christ, C. M.., 1965. Solutions, Minerals, and Equilibria. Harper Geoscience Series. Harper and Row, New York, 465pp.G.K. Gilbert, 1909. The convexity of hilltops. J. Geology, 17, 344-351.

Goddéris Y., François, L.M., Probst, A., Schott, J., Moncoulon, D., Labat, D., and Viville, D., 111 2006. Modelling weathering processes at the catchment scale: The WITCH numerical 112 model. Geochimica et Cosmochimica Acta 70, 1128-1147

Hamdan, J & \Burnham, C.P., 1996. The contribution of nutrients from parent material in three deeply weathered soils of Peninsular Malaysia. Geoderma 74, 219-233.

Heimsath, A.M. Dietrich, W.E., Nishiizumi, K., and Finkel, R.C.., 1997. The soil production function and landscape equilibrium. Nature, 388: 358-361

. Hernández-Soriano M. C. 2012. The Role of Aluminum-Organo Complexes in Soil Organic Matter Dynamics. In Dynamics, Soil Health and Land Use Management, Dr. Maria C. Hernandez Soriano (Ed.), ISBN: 978-953- 307-614-0

. Hoosbeek M.R & Bryant, R.B., 1994. Developing and adapting soil process sub-models for use in the pedodynamic Orthod model. In Quantitative Modeling of Soil Forming Processes. SSSA Special Publication 39, pp 111-128.

Johnson M O.,. Mudd S M Pillans, ,B. Spooner, N A Fifield, L. K Kirkby M J. and Gloor, M 2014. Quantifying the rate and depth dependence of bioturbation based on optically-stimulated luminescence (OSL) dates and meteoric 10Be. Earth Surf. Process. Landforms 39, 1188–1196

Kirkby, M.J, 1967. Measurement and theory of soil creep, J. Geology 75, 359-378.

Kirkby, M.J,.1977. Soil development models as a component of slope models. Earth Surface Processes, 2, 203-30.

Kirkby M.J., 1985a. The basis for soil profile modelling in a geomorphic context. J. Soil Science 36, 97-121.

. Kirkby, M.J 1985b. A model for the evolution of regolith-mantled slopes, in Models in geomorphology, ed M.J. Woldenburg, Allen & Unwin, 213-37.

. Li, D.D ,Jacobson, A.D., & McInerney, D.J.,2014. A reactive-transport model for examining tectonic and climatic controls on chemical weathering and atmospheric CO2 consumption in granitic regolith. Chemical Geology, 365, 30-42.

Lebedeva, M.I., Fletcher, R.C. and S.L. Brantley, S.L., 2010. A mathematical model for steady-state regolith production at constant erosion rate. Earth Surf. Process. Landforms 35, 508–524

. McTeague J.A & Cline, M.G., 1962.Silica in soil solutions. II The adsorption of monosilicic acid by soil and by other substances. Canadian Journal of Soil Science, 43, 83-96.

Minasny B. and McBratney, A.B., 1999. A rudimentary mechanistic model for soil production and landscape development. Geoderma 90, 3–21.

Minasny B.and McBratney, A.B., 2001. A rudimentary mechanistic model for soil formation and landscape development: II. A two-dimensional model incorporating chemical weathering. Geoderma 103, 161–179.

Opolot, E., Finke, P.A. 2015 Evaluating sensitivity of silicate mineral dissolution rates to physical weathering using a soil evolution model (SoilGen2.25). *Biogeosciences* 12: 6791-6808.

Riebe C. S.,. Kirchner J. W &. Finkel R. C, 2003. Long-term rates of chemical weathering and physical erosion from cosmogenic nuclides and geochemical mass balance. Geochimica et Cosmochimica Acta, 67, 4411–4427.

Robinson R. A. and. Stokes R. H, 1959. Electrolyte solutions. Academic Press, New York, 559 pp

Terzaghi K.&. Peck, R.P 1967. Soil Mechanics in Engineering Practice. John Wiley, New York, 729pp.

Van Genuchten M. Th & Wierenga, P.J., 1986.Solute dispersion coefficients and retardation factors. In Klute (ed) methods of Soil Analysis, Part I. Agronomy Monographs 9, ASA and SSSA, madison ,WI, pp1025-1054.

Vanwalleghem T., Stockmann, U., Minasny, B., McBratney, A.B., 2013. A quantitative model for integrating landscape evolution and soil formation. J. Geophys. Res. Earth Surf. 118, 1–17.

. Welivitiya, W.D.D. P., Willgoose G.R.,. Hancock G.R & Cohen S., 2016.Exploring the sensitivity on a soil area-slope.grading relationship to changes in process parameters using a pedogenesis model. Earth Surface Dynamics 4, 607-625. doi:10.5194/esurf-4-607-2016

Willgoose, G.R., 2018. Principles of soilsscape and landscape evolution, Cambridge University Press.

Component oxide	Al	Si	Ca	Mg	Na	K	Fe	Ti	Total (%)	Solubility (mg/l)
Initial p	14.0	49.0	7.0	13.0	1.7	0.3	13.0	2.0	**100**	**20.3**
solubility (mg/l)	6	15	80	40	60	0.2	2	0		
Relative time										
0	14.0	49.0	7.0	13.0	1.7	0.3	13.0	2.0	**100**	**20.3**
10	13.2	42.2	3.1	8.7	0.9	0.3	12.7	2.0	**83**	**13.9**
20	12.4	36.3	1.4	5.8	0.5	0.3	12.5	2.0	**71**	**10.2**
30	11.7	31.2	0.6	3.9	0.3	0.3	12.2	2.0	**62**	**7.9**
40	11.0	26.9	0.3	2.6	0.2	0.3	12.0	2.0	**55**	**6.3**
50	10.4	23.1	0.1	1.8	0.1	0.3	11.8	2.0	**50**	**5.2**
60	9.8	19.9	0.1	1.2	0.0	0.3	11.5	2.0	**45**	**4.4**
70	9.2	17.1	0.0	0.8	0.0	0.3	11.3	2.0	**41**	**3.7**
80	8.7	14.8	0.0	0.5	0.0	0.3	11.1	2.0	**37**	**3.2**
90	8.2	12.7	0.0	0.4	0.0	0.3	10.9	2.0	**34**	**2.8**
100	7.7	10.9	0.0	0.2	0.0	0.3	10.6	2.0	**32**	**2.4**

Table 1: Illustration of progressive linear solution of rock material. See also figure 3.

Parameter description	Range of values	Units	Symbol	Comment
Solute concentration at p=1	1-100	mg. l^{-1}	c_*	c_* in equation (5)
Solute exponent	0.5			Exponent in equation (5)
Precipitation	100-2000	mm. a^{-1}	P	
Potential evapotranspiration	200-2000	mm. a^{-1}	E_P	Actual ET calculated as $1/\sqrt{(1/P^2+1/E_P^2)}$
Depth of ET penetration	20-200	mm		Depth in soil
Mechanical denudation at p=0	0.1-100	mm/ Ka^{-1}	M_0	In equation (10)
Exponent for mechanical denudation	0.1			Exponent in equation (10)
Capacity for lateral subsurface flow increment at p=0	50-1000	mm. a^{-1}		Should be proportional to slope profile convexity
Lower limit of weathering	0.4-0.8		p_0	Proportion remaining can never be less than this limit value
Reduction in solute removal at surface	1			Can allow for reduced solute loss in overland flow
Ionic diffusion rate	1-100	cm^2. a^{-1}	K_I	Dominant near parent material
Bioturbation diffusion rate	1-100	cm^2. a^{-1}	K_B	Dominant near surface
Depth of bioturbation penetration	20-200	mm		Depth in soil
Additional percolation capacity for parent material	0	mm. a^{-1}		Not operational

523 **Table 2: Example Model parameters**

524

Figure captions

1. Hydrological, chemical, biological and mechanical processes within the critical zone
2. Definition sketch: a generalised soil profile.
3. Linear solution example.
    a. Initial assumed composition
    b. Composition after weathering to p=0.4
    c. Relationship between average solubility and proportion remaining
    d. Proportion remaining for three components over time

4. Components of soil development for steady state case of equation 9, with no bioturbation

    a. Shows fluxes due to ionic diffusion and advection

    b. Shows net gains or losses. The region of greatest change corresponds to the migrating weathering front in which p is changing most rapidly.

5. Example of soil profile evolution in the model.

Modelled decline in solution rate with soil deficit (~ depth) over 300Ka. Values taken from model run shown in figure 5.

6. Evolution of soil deficit over time for a range of climates from humid to arid. The legend shows the precipitation and potential ET (in mm per year) for each model run. Values in the legend are the ratios of precipitation to Pot ET.
7. Model runs that differ only in the initial rate of potential mechanical denudation. The upper curves show the modelled evolution of mechanical and chemical denudation. The lower curve shows the final equilibrium states (not reached in some cases). In which $p_s=M/(M+C)$.
8. The almost single-valued relationship between soil deficit (or generalised soil depth) and the degree of weathering at the surface, ζ =f(ps), for the set of model runs shown in figure 8.
9. Simplified soil profile evolution model, using equations 6, 10-12. Note that total denudation greatly exceeds soil deficit.
10. Embedding soil profile model within a landscape evolution model
11. Tentative identification of climatic regions with the composite variable $\log(E_A)+ \log(r/R)$ as an indicator of regional final state of weathering, p_0. E_A is actual evapotranspiration, r/R is the ratio of runoff to precipitation, the reciprocal of aridity. The axes of the plot are for annual precipitation and mean annual temperature. Values on the graph indicate suggested values for p_0.

565

Biologically active zone

Chemically active zone

Bedrock

Evapotranspiration

Hydrology

Precipitation

Infiltration
Lateral flow

Root uptake

Minimal flow

+/- Static Saturated

Advection of water & solutes……throughout

Chemistry

(Rock constituents)
Leaf-fall

Selective root uptake

Declining activity

Ionic diffusion

Biology

(SOM and pCO2 profiles)

Leaf-fall

Root-fall

Biotrubation

Mechanical

Frost heave/ wetting drying

Lateral Sediment transport at rates that generally decrease with depth below surface

Dilation with reduction in overburden

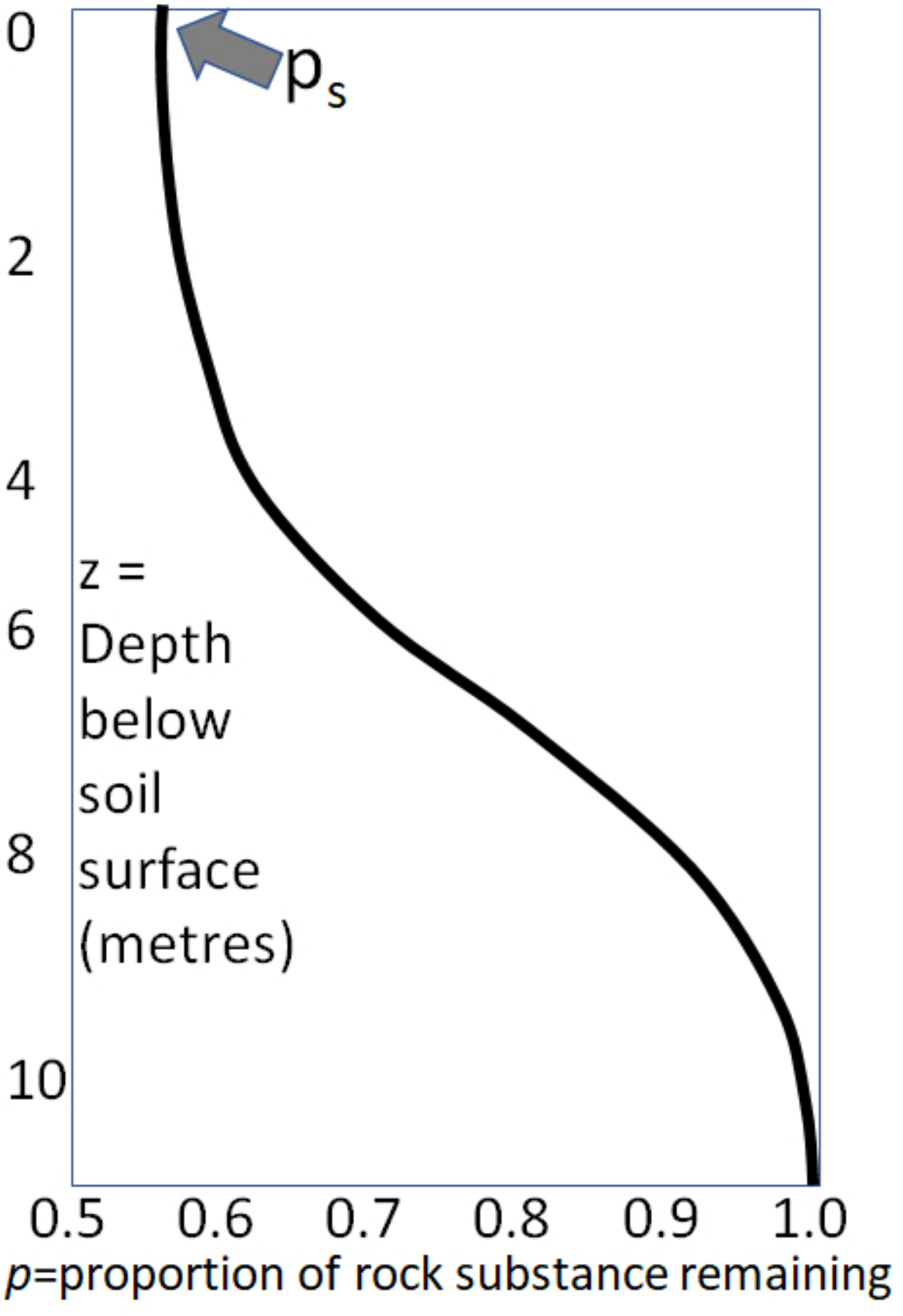
0
2
4
6
8
10
p_s
z =
Depth
below
soil
surface
(metres)
0.5
0.6
0.7
0.8
0.9
1.0
p=proportion of rock substance remaining

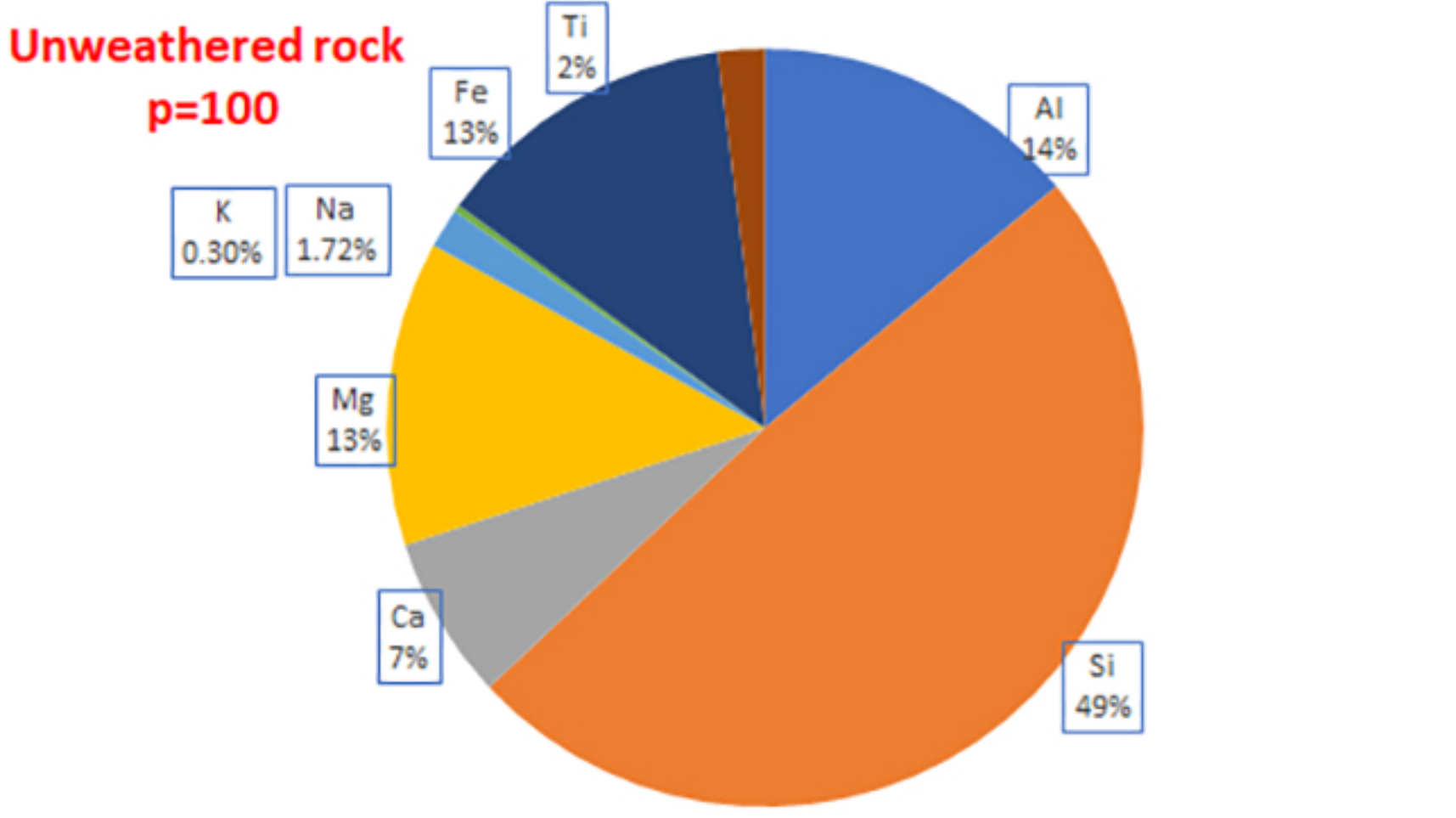
Unweathered rock
p=100
Ti
2%
Fe
13%
Al
14%
K
0.30%
Na
1.72%
Mg
13%
Ca
7%
Si
49%

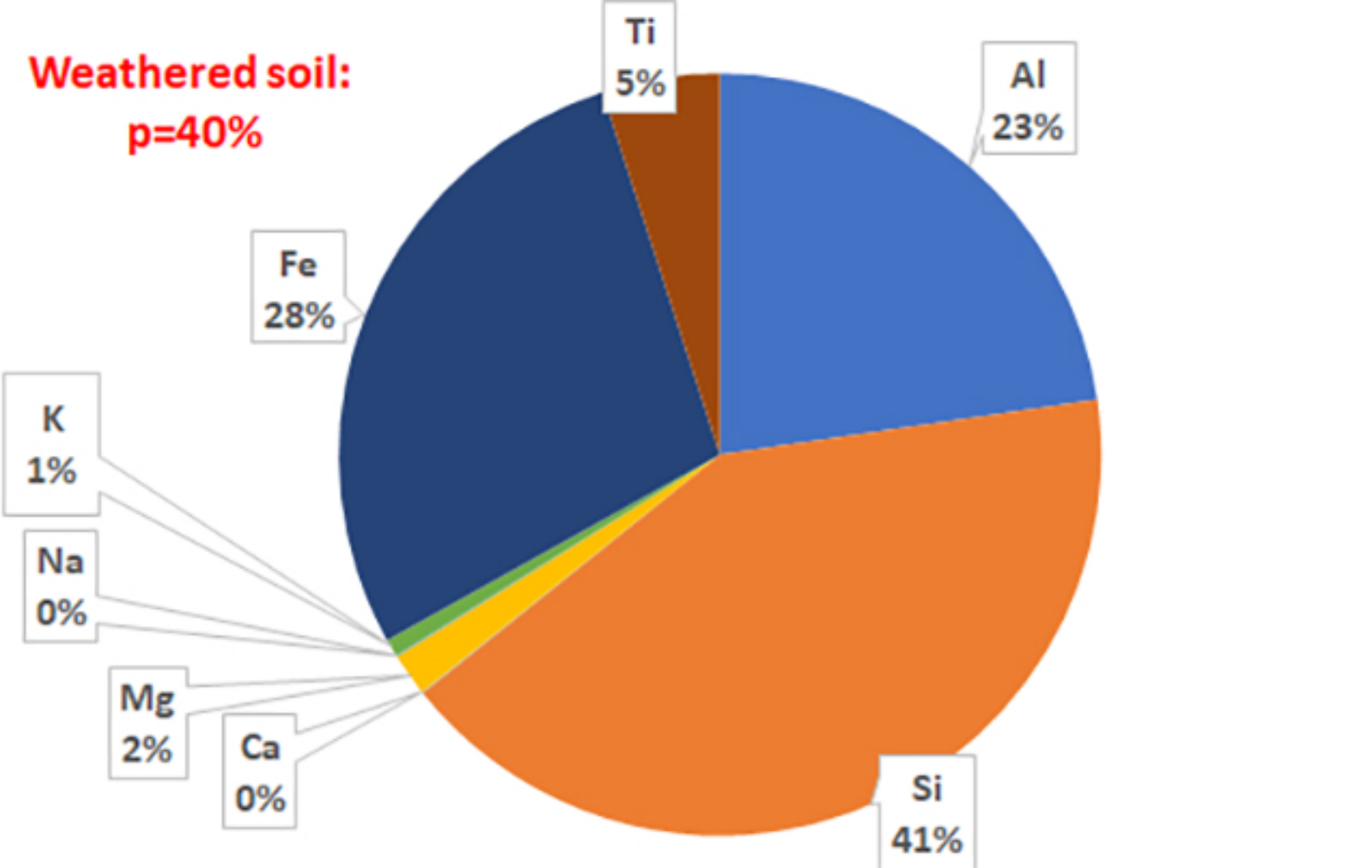
Weathered soil:
p=40%
Ti
5%
Al
23%
Fe
28%
K
1%
Na
0%
Mg
2%
Ca
0%
Si
41%

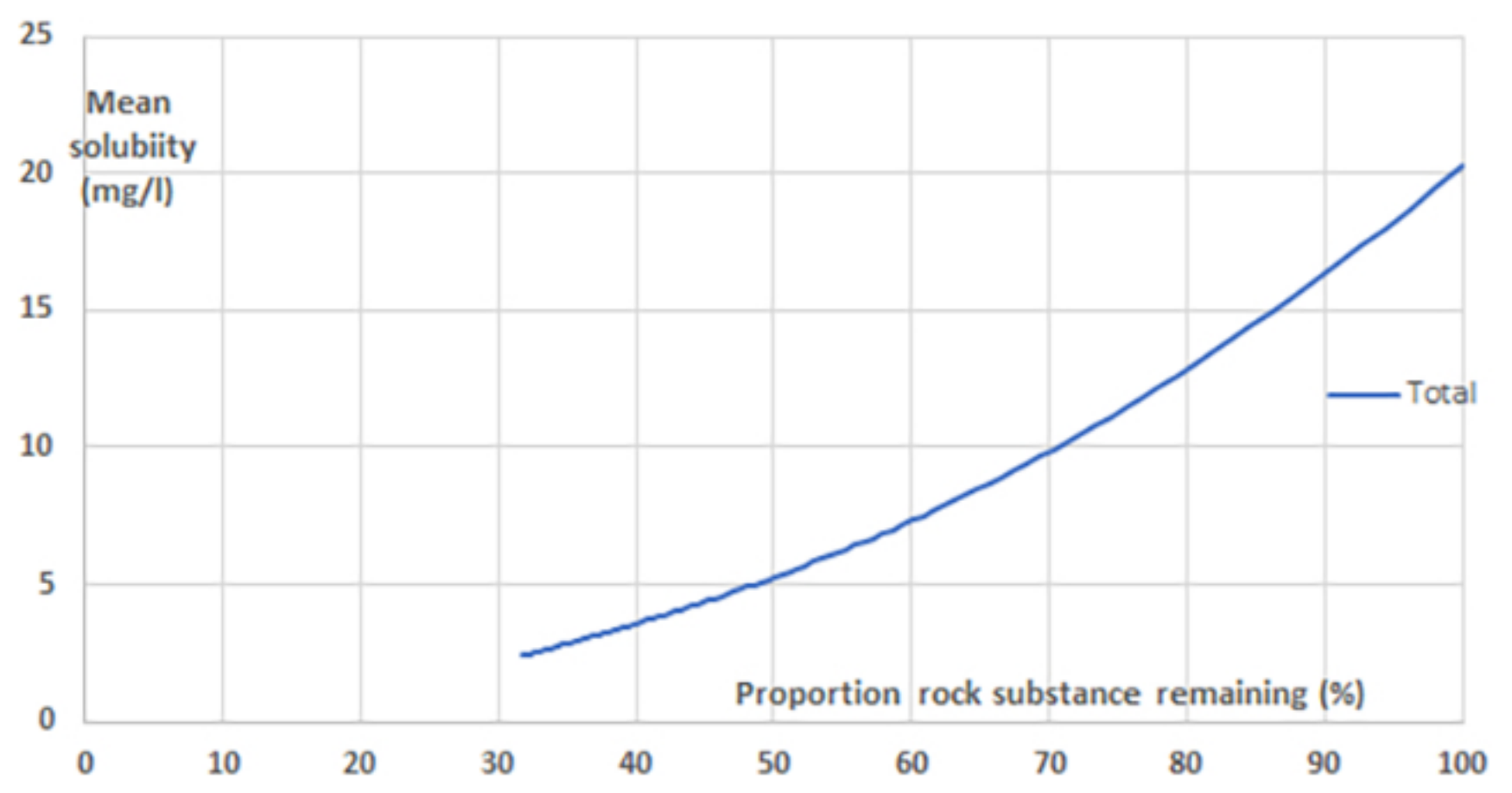
Mean solubiity (mg/l)
25
20
15
10
5
0
Total
Proportion rock substance remaining (%)
0
10
20
30
40
50
60
70
80
90
100

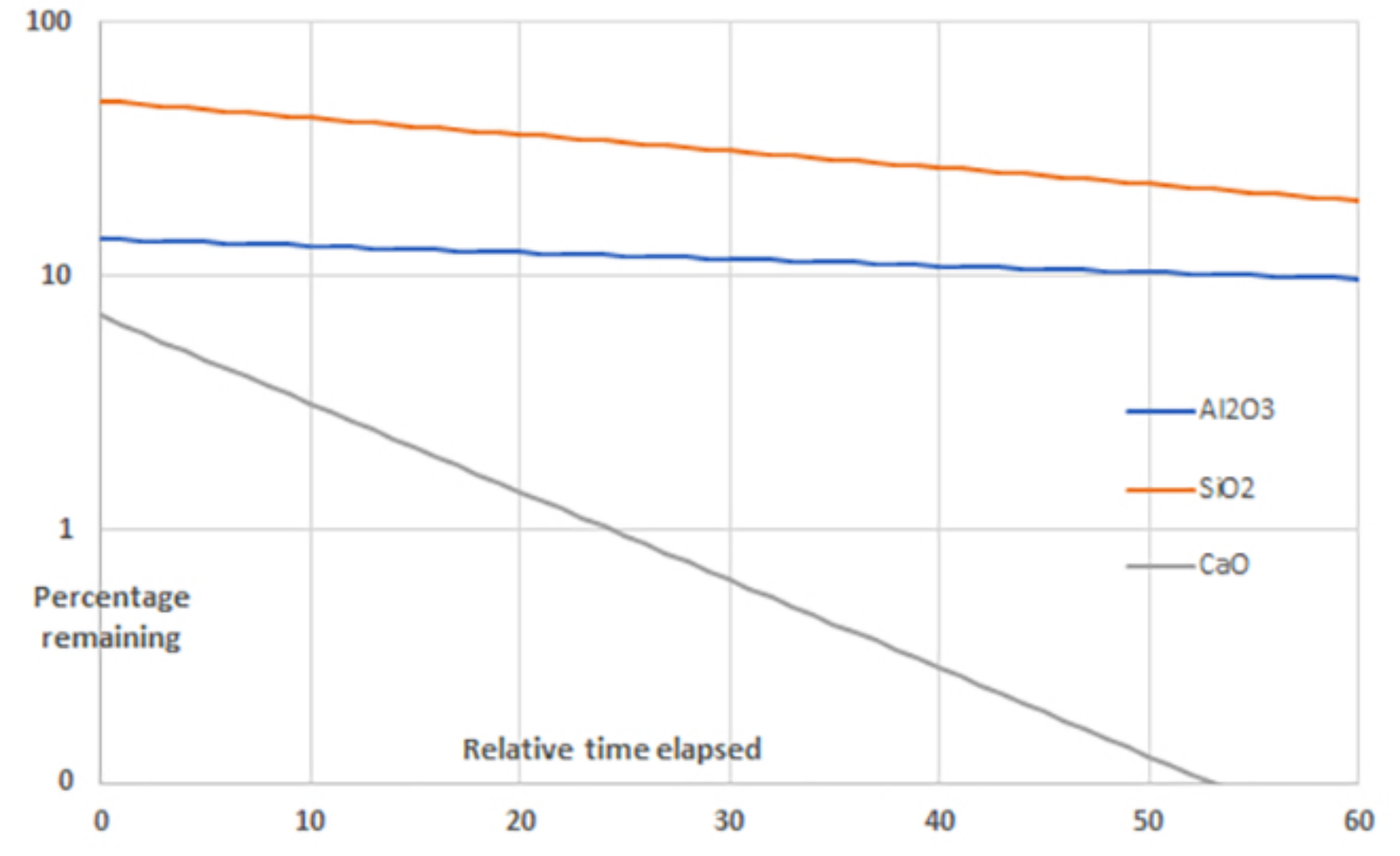
100
10
1
0
Percentage remaining
Relative time elapsed
0
10
20
30
40
50
60
Al2O3
SiO2
CaO

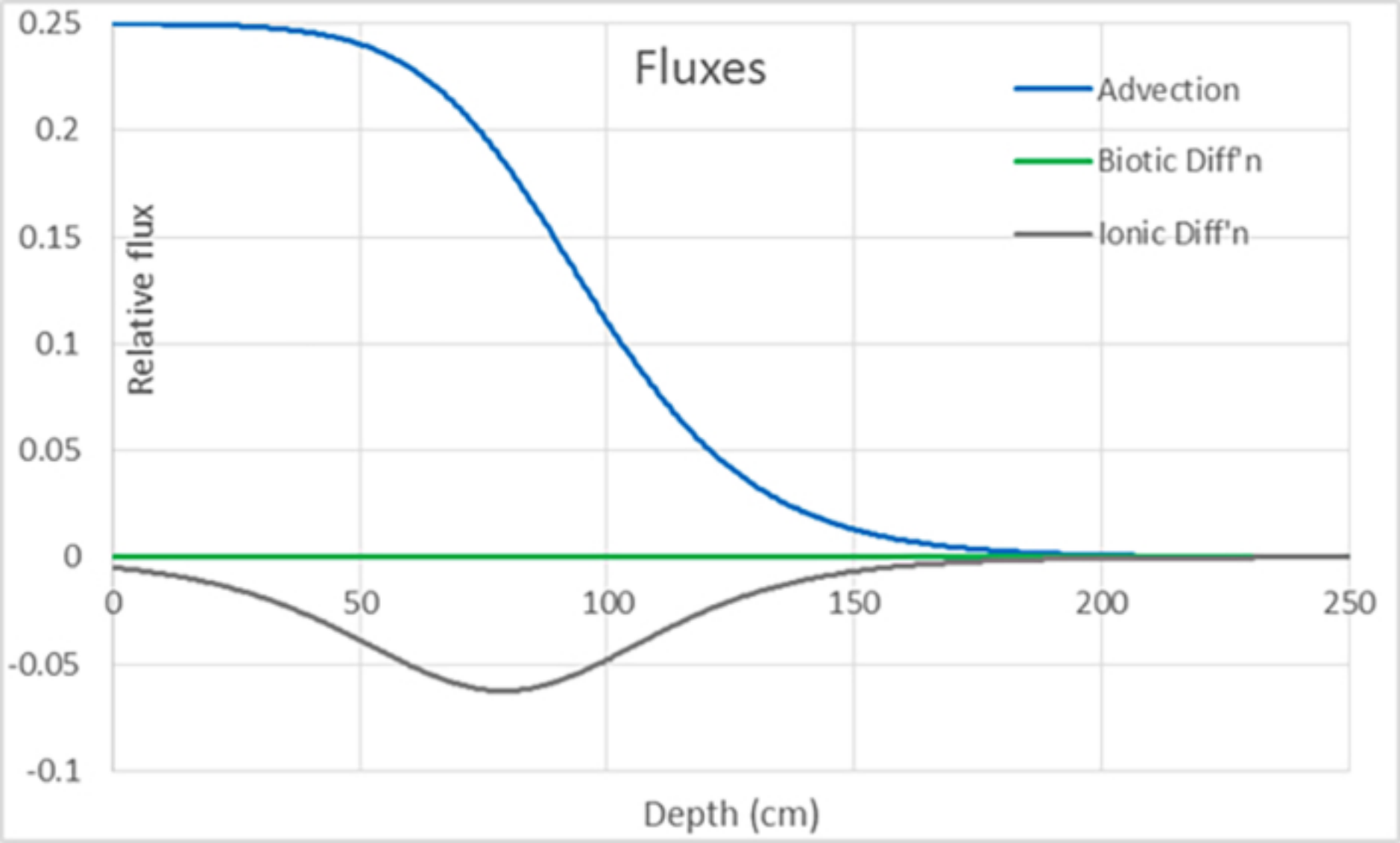
Fluxes
Advection
Biotic Diff'n
Ionic Diff'n
Relative flux
0.25
0.2
0.15
0.1
0.05
0
-0.05
-0.1
0
50
100
150
200
250
Depth (cm)

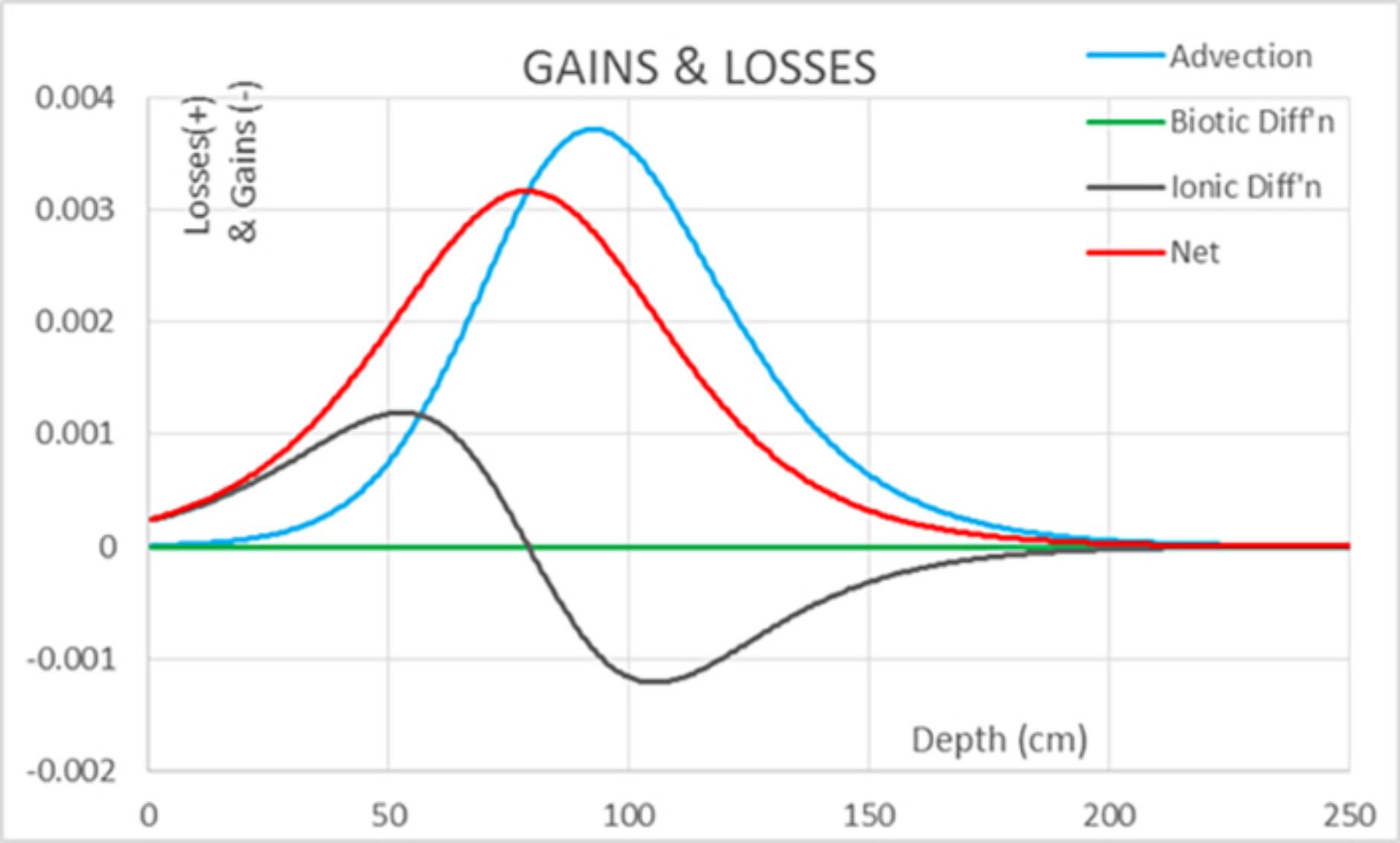
GAINS & LOSSES
Advection
Biotic Diff'n
Ionic Diff'n
Net
Losses(+) & Gains(-)
0.004
0.003
0.002
0.001
0
-0.001
-0.002
Depth (cm)
0
50
100
150
200
250

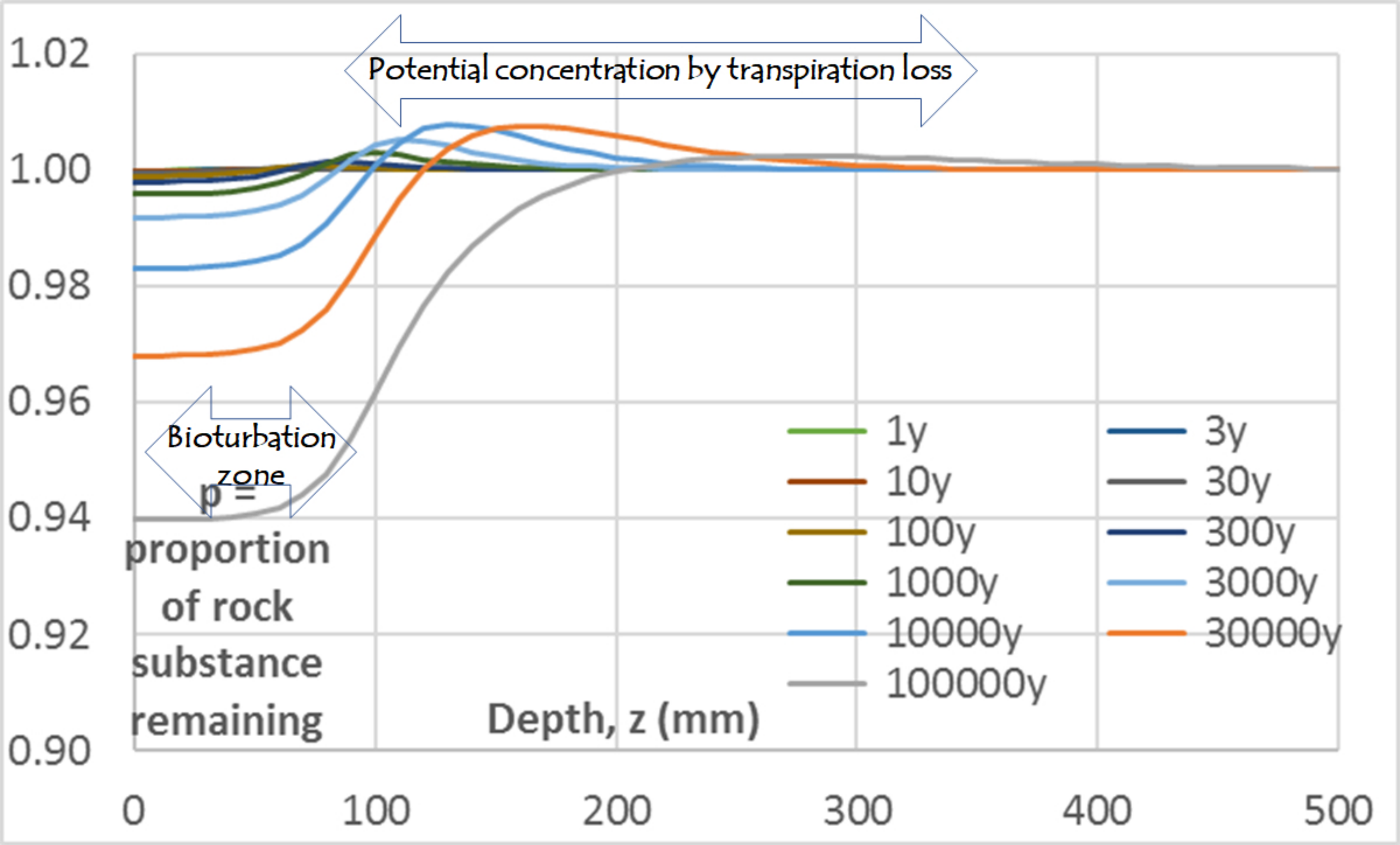
Potential concentration by transpiration loss
Bioturbation zone
p =
proportion of rock substance remaining
Depth, z (mm)
1y
3y
10y
30y
100y
300y
1000y
3000y
10000y
30000y
100000y
1.02
1.00
0.98
0.96
0.94
0.92
0.90
0
100
200
300
400
500

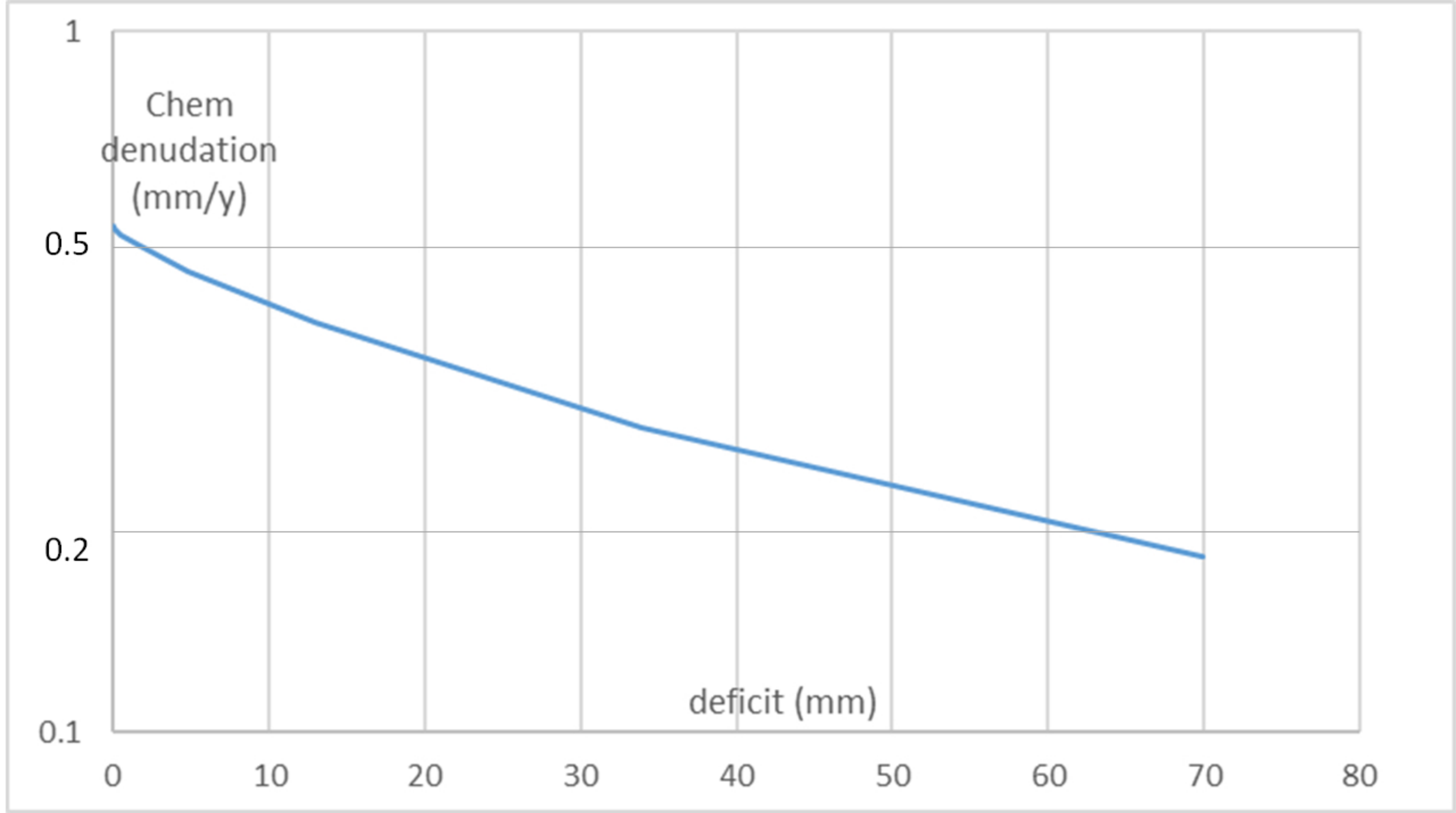
1
Chem denudation (mm/y)
0.5
0.2
0.1
deficit (mm)
0
10
20
30
40
50
60
70
80

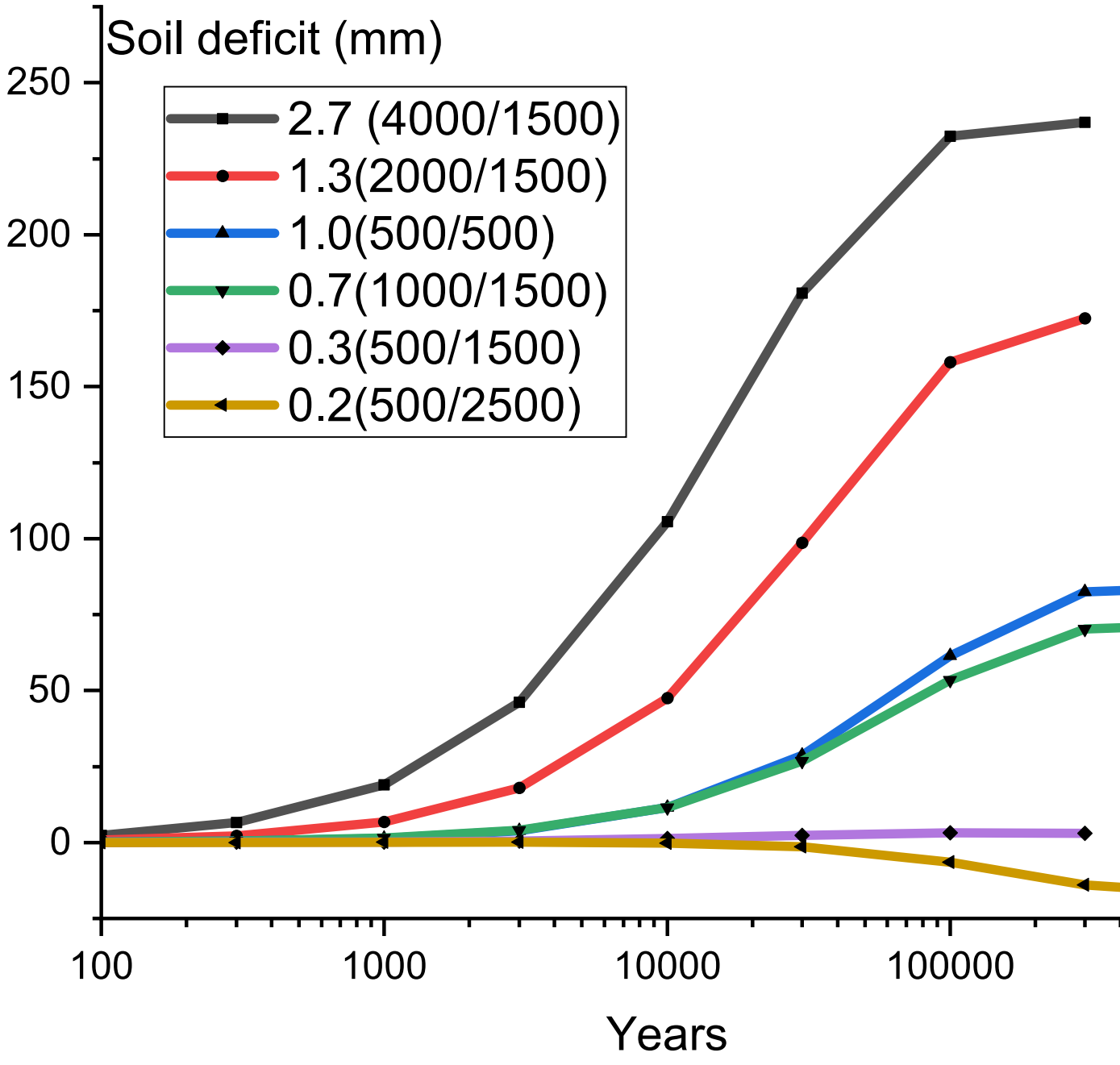
Soil deficit (mm)
250
200
150
100
50
0
2.7 (4000/1500)
1.3(2000/1500)
1.0(500/500)
0.7(1000/1500)
0.3(500/1500)
0.2(500/2500)
100
1000
10000
100000
Years

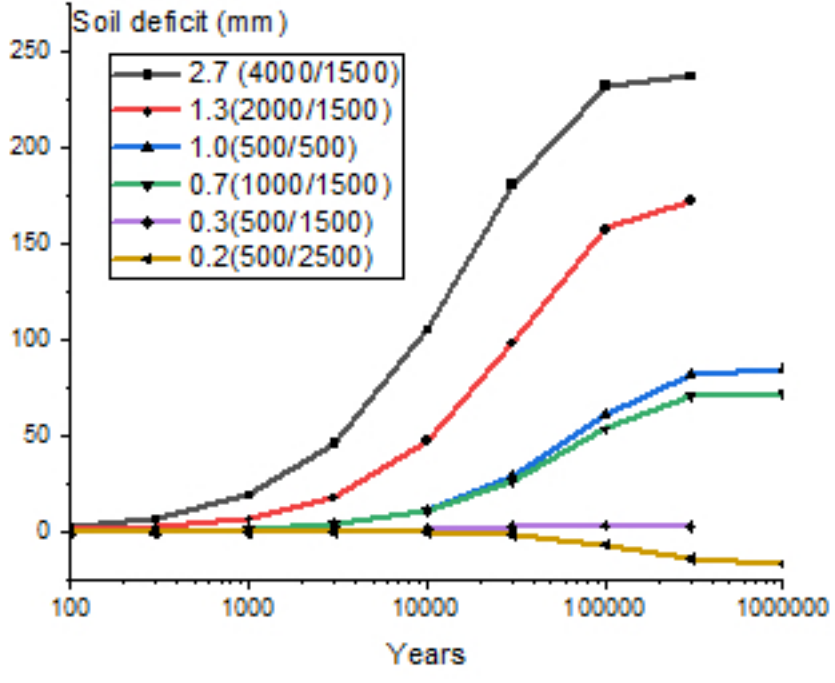
Soil deficit (mm)
2.7 (4000/1500)
1.3(2000/1500)
1.0(500/500)
0.7(1000/1500)
0.3(500/1500)
0.2(500/2500)
250
200
150
100
50
0
100
1000
10000
100000
1000000
Years

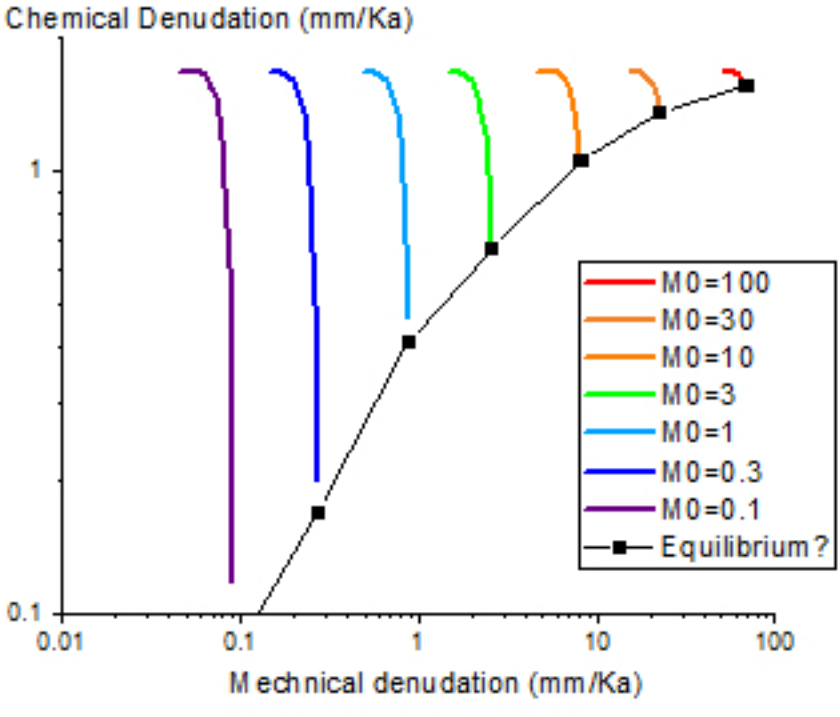
Chemical Denudation (mm/Ka)
1
0.1
0.01
0.1
1
10
100
Mechnical denudation (mm/Ka)
M0=100
M0=30
M0=10
M0=3
M0=1
M0=0.3
M0=0.1
Equilibrium?

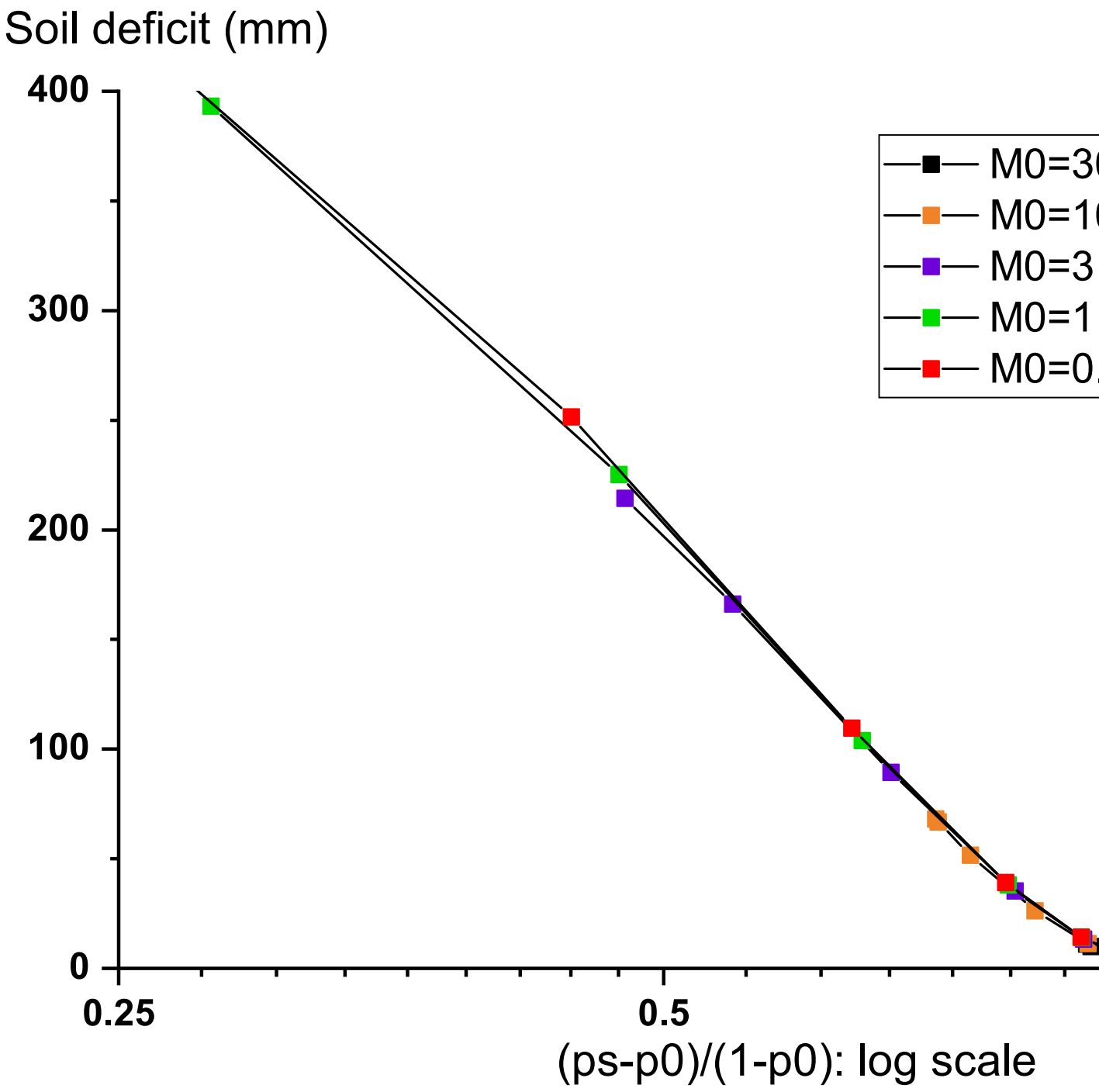
Soil deficit (mm)
400
300
200
100
0
0.25
0.5
(ps-p0)/(1-p0): log scale
M0=3
M0=1
M0=3
M0=1
M0=0

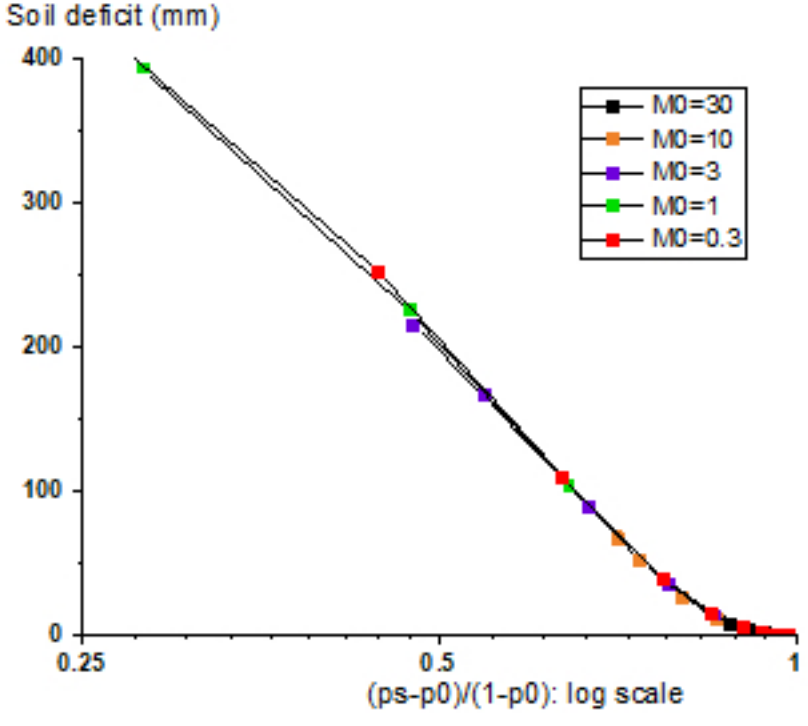
Soil deficit (mm)
400
300
200
100
0
0.25
0.5
1
(ps-p0)/(1-p0): log scale
M0=30
M0=10
M0=3
M0=1
M0=0.3

Soil deficit (mm)
Denudation rate (mm/Ka)
p_s (Right hand scale)
Soil deficit/ denudation rate
ps
300
250
200
150
100
50
0
1
0.9
0.8
0.7
0.6
0.5
0.4
0.3
0.2
0.1
0
0
2
4
6
8
10
12
14
16
18
20
Time Ka

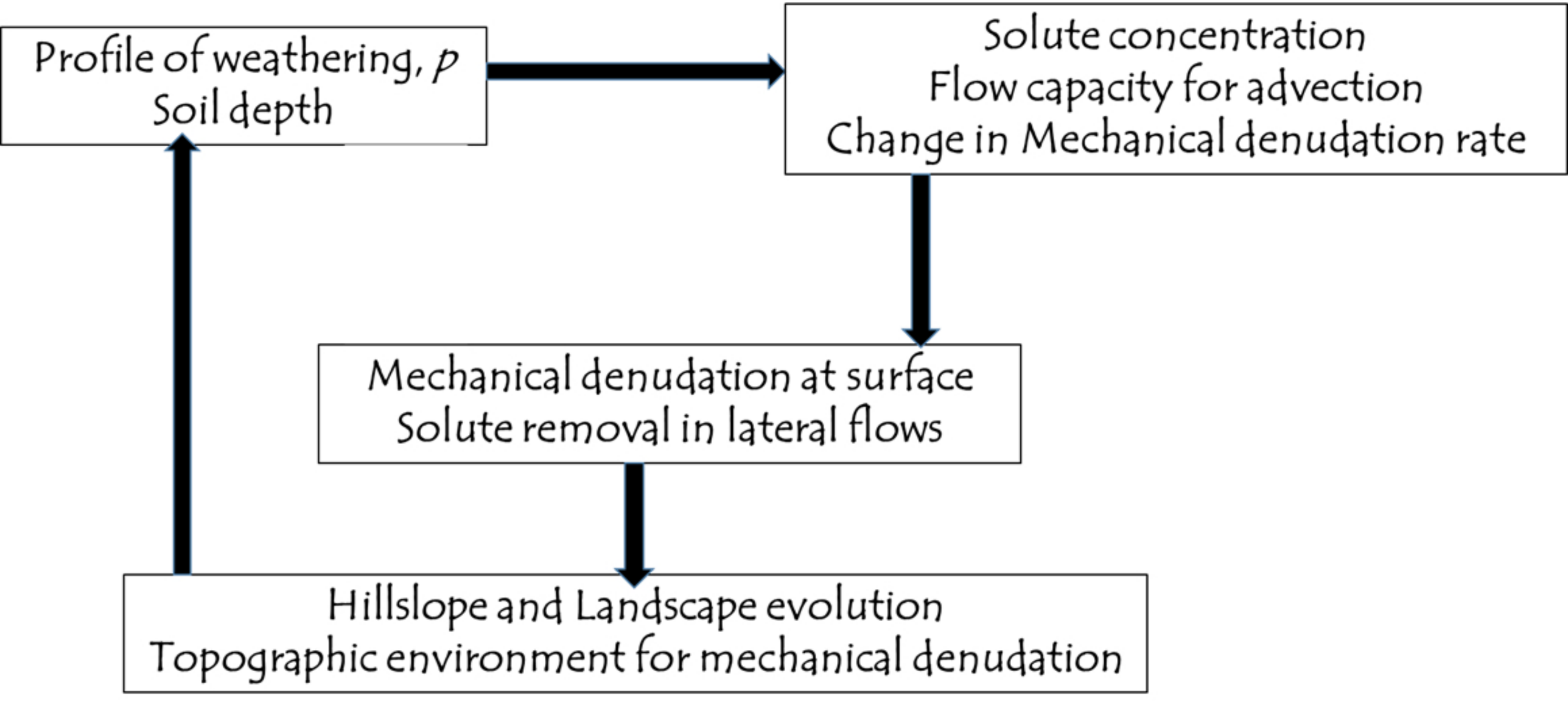
Profile of weathering, p
Soil depth
Solute concentration
Flow capacity for advection
Change in Mechanical denudation rate
Mechanical denudation at surface
Solute removal in lateral flows
Hillslope and Landscape evolution
Topographic environment for mechanical denudation

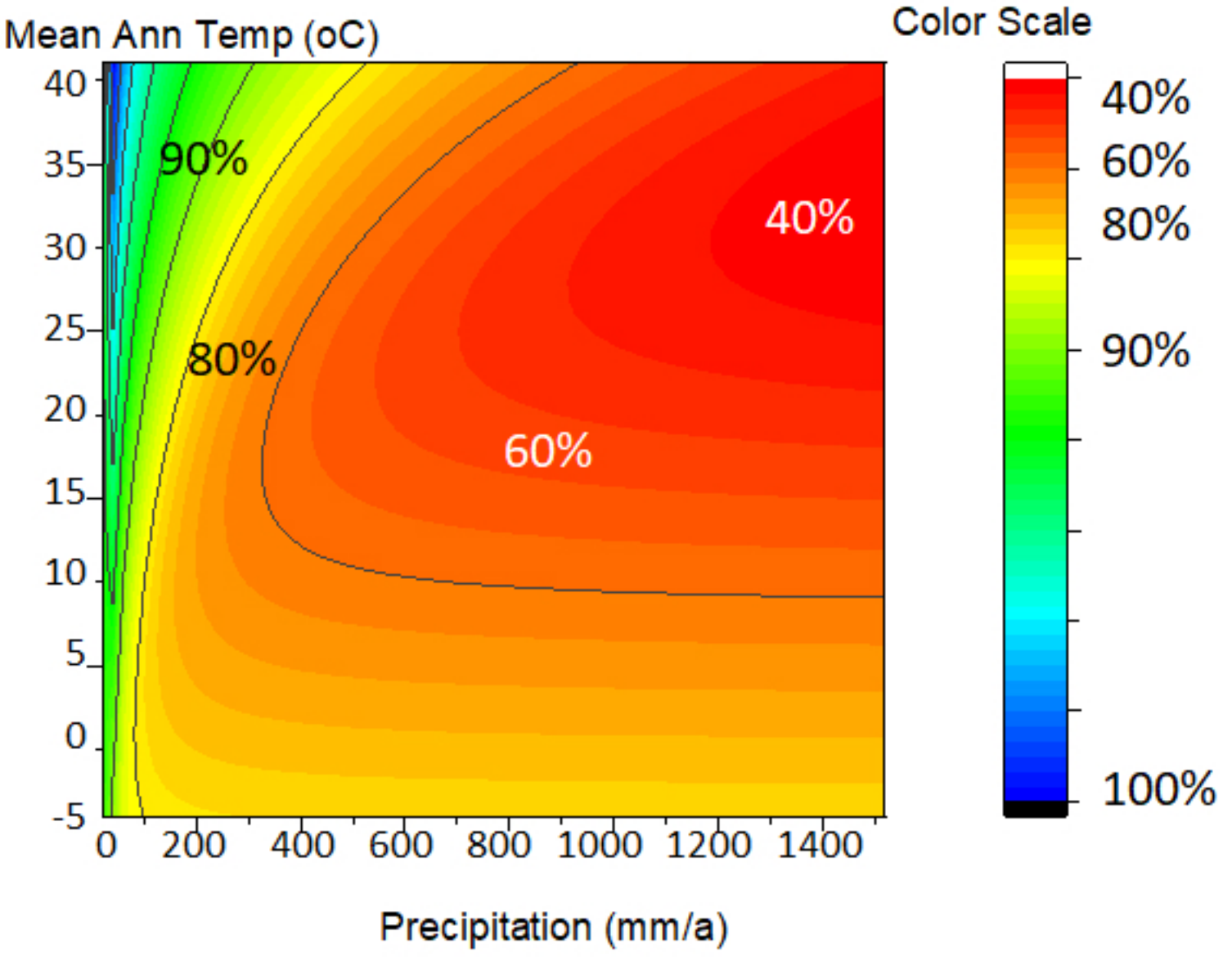
Mean Ann Temp (oC)
40
35
30
25
20
15
10
5
0
-5
0
200
400
600
800
1000
1200
1400
Precipitation (mm/a)
90%
80%
60%
40%
Color Scale
40%
60%
80%
90%
100%